Osmotically Driven Shape Transformations in Axons

Pramod A. Pullarkat,[1] Paul Dommersnes,[2] Pablo Fernández,[1] Jean-François Joanny,[2] and Albrecht Ott[1]

[1]*Experimentalphysik I, University of Bayreuth, D-95440, Bayreuth, Germany*
[2]*Institut Curie, UMR 168, 26 rue d'Ulm, F-75248, Paris Cedex 05, France*

(Received 8 July 2005; published 2 February 2006)

We report a cylindrical-peristaltic shape transformation in axons exposed to a controlled osmotic perturbation. The peristaltic shape relaxes and the axon recovers its original geometry within minutes. We show that the shape instability depends critically on the swelling rate and that volume and membrane area regulation are responsible for the shape relaxation. We propose that volume regulation occurs via leakage of ions driven by elastic pressure, and analyze the peristaltic shape dynamics taking into account the internal structure of the axon. The results obtained provide a framework for understanding peristaltic shape dynamics in nerve fibers occurring *in vivo*.

DOI: 10.1103/PhysRevLett.96.048104 PACS numbers: 87.16.−b, 47.20.Dr, 87.19.La

Axons and dendrites, collectively known as neurites, are thin, tubular extensions produced by neuronal cells [1]. Structurally, they consist of an outer lipid membrane sheath bound to a core made up of an elastic network of highly cross-linked biopolymers known as the cytoskeleton. Neurites are known to lose their normal cylindrical geometry and become peristaltically modulated—a process commonly known as beading—under a wide range of situations. These include neurodegenerative diseases like Alzheimer's [2], brain trauma [3], stretch injuries to nerves [4], and *in vitro* as well as *in vivo* application of neurotoxins or drugs [5], among others. In stretch injuries, tension in the axon is responsible for beading. In the other examples, disruption of cytoskeletal integrity appears to be a common feature.

Peristaltic modes have been studied in tubular membranes and gels under tension [6–8]. This ''pearling instability'' is driven by surface tension, as in the Rayleigh-Plateau instability of liquid columns [9]. In liquid columns, peristaltic perturbations with wavelengths larger than the circumference grow as they reduce surface area at constant volume. Unlike liquid columns, cylindrical vesicles or gels are unstable only beyond a critical tension, when the gain in surface energy due to a reduction in area overcomes the elastic energy for deforming the membrane or gel. Similar arguments can explain peristaltic modes observed in stretched nerves [10] and cell protrusions exposed to toxins [11]. In all the above-mentioned biological examples the beaded state persists and no recovery has been observed.

We report a novel, reversible, peristaltic instability observed in chick-embryo axons and in PC12 neurites [12] after a sudden dilution of the external medium, as shown in Fig. 1. The transition to the peristaltic state occurs at a threshold membrane tension, induced by osmotic swelling. However, unlike previous reports on beading, the osmotically induced instability relaxes and the neurite recovers its original shape within minutes. We show that the relaxation is due both to cell volume and membrane surface regulation. Remarkably, the shape stability depends critically on the swelling rate. We model the pearling-beading instability taking into account the gel-like dynamics of the cytoskeleton and the membrane-cytoskeleton coupling, and find wavelengths in agreement with experimental observations. Further, we propose that elastic stresses in the cytoskeleton provide the driving force for water and ions to leak through channel proteins in the membrane [1] to effect volume regulation.

Experiments.—The experiments are performed using a $10 \times 5 \times 1$ mm^3 flow chamber with temperature maintained within ± 0.2 °C. The cells are grown on treated glass coverslips [12] and transferred to the flow chamber. The flow velocity in the plane of the axon is about 1 μm s^{-1} and the shear rate is about 1 s^{-1}, well below values needed to cause any significant shear stress on the neurites. The flow is switched from normal medium, with an ion concentration $\phi_0 = 0.3$ mol/l, to a diluted medium to induce a hyposmotic shock. Phase contrast images are recorded using a CCD camera at a magnification of 0.084 μm/pixel. The neurite boundaries are traced with a typical error of a couple of pixels using a home-developed image analysis software. The volume and area are computed assuming axial symmetry. Only neurites that are firmly adherent at the two ends and freely suspended along the length are used for measurements.

After exposure to a hyposmotic solution, the neurite immediately starts to swell with a uniformly increasing

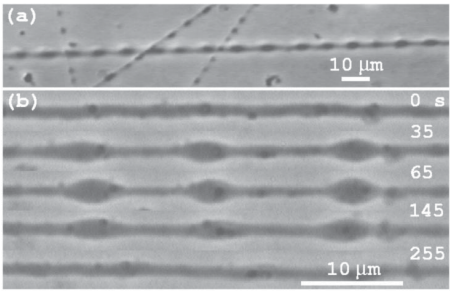

FIG. 1. (a) Osmotically induced shape instability in chick-embryo neurons. (b) Image sequence showing the growth and relaxation of the instability in a PC12 neurite.

radius from its initial value R_0. Figure 2 shows the typical variation of the normalized volume $\tilde{V} = V/V_0$ and area $\tilde{A} = A/A_0$. For sufficiently large osmotic shocks, a standing peristaltic mode sets in at a threshold radius R_c. The plot of $\sqrt{\tilde{V}}/\tilde{A}$ shows the evolution of the peristaltic shape. An increase in $\sqrt{\tilde{V}}/\tilde{A}$ indicates a reduction in surface area compared to a cylinder with identical volume. The mode amplitude increases with time, reaches a maximum, and then decreases back to zero. The amplitude and the wavelength appear uniform along the entire length of the neurite (see Fig. 1). An analysis of the instability observed on more than a hundred PC12 neurites with lengths of ~50–500 μm reveals the following. (i) The instability occurs only above a critical dilution, which is about $0.5\phi_0$ at 37 °C and about $0.7\phi_0$ at 25 °C for an initial radius $R_0 \simeq 0.7$ μm. The critical dilution decreases for smaller R_0 or for lower temperature. (ii) The wavelength λ increases with increasing R_0 but is independent of the neurite length. For a given neurite, the wavelength remains approximately constant during both the growth and relaxation of the instability. (iii) The maximum volume V_m scales linearly with V_0; i.e., V_m/V_0 is largely independent of the neurite selected. (iv) Typically, the instability sets in when the area increases by 3%–8%. The maximum increase can reach 20%. (v) For osmotic shocks slightly below the critical value, no shape change occurs even when the area increases well beyond the 3%–8% mentioned earlier. The growth rate of the area decreases with decreasing osmotic shock. Therefore, we conclude that the stability depends on the rate of area increase as well as its magnitude. In another set of experiments, when the dilution is performed in several steps of very weak osmotic shocks, the neurites remain cylindrical even when the external solution is diluted to pure water. In this case the volume and area remain close to their initial values throughout the experiment. (vi) Water flow across the membrane is mainly through water specific channel proteins belonging to the aquaporin family [13]. Blocking them using 500 mM dimethylsulfoxide significantly reduced swelling and made the neurites more resistant to peristaltic shape change.

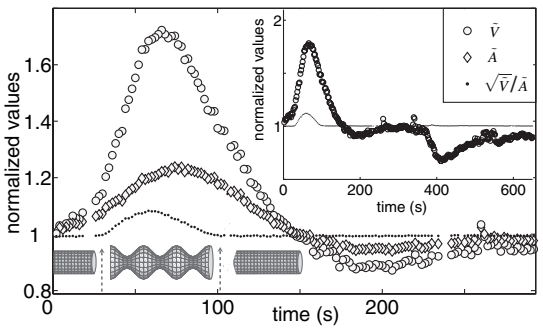

FIG. 2. Evolution of the normalized volume $\tilde{V}$ and area $\tilde{A}$ of a neurite with $R_0 = 0.5$ μm at 33 °C. The ratio $\sqrt{\tilde{V}}/\tilde{A}$ (dotted line) reflects any deviations from the cylindrical geometry. The inset shows the volume and shape responses when the concentration is switched in the sequence $\phi_0 \overset{0\ \mathrm{s}}{\rightarrow} 0.5\phi_0 \overset{370\ \mathrm{s}}{\rightarrow} \phi_0$. The initial slow swelling is due to a nonsteplike change in concentration, as revealed by using an absorbing dye. Note: the shape remains cylindrical for the $0.5\phi_0 \rightarrow \phi_0$ shock.

Discussion.—*Volume regulation:* We assume the neurite to be a cylindrical, isotropic gel with an adhering fluid membrane on its surface. Based on fluorescence microscopy, we conclude that the membrane is firmly attached to the cytoskeleton at least during the onset of the instability. The osmotic pressure difference across the membrane is $\Delta\Pi = kT(\phi_i - \phi_e)$, where ϕ_e and ϕ_i are the external and internal net ion concentrations. The volume flux of water through the membrane is

$$J_w = L_p(\Delta\Pi - \Delta p), \tag{1}$$

where L_p is the membrane permeability to water and Δp is the hydrodynamic pressure difference over the membrane. The gel response time is faster than the time scale of swelling, which is determined by L_p. The local normal force balance at the membrane determines the hydrodynamic pressure jump $\Delta p = (K + 4\mu/3)\Delta R/R_0 + E\Delta R/R_0^2 = \tilde{K}\Delta R/R_0$, where $R = R_0 + \Delta R$ is the neurite radius, K and μ are the compression and shear moduli, and E is the stretching modulus of the membrane. The volume growth rate of the neurite is $\dot{V} = J_w A$.

Volume relaxation occurs due to the opening of membrane-bound ion-channel proteins [1]. This regulatory volume decrease is known to involve both "active" as well as "passive" processes, many of which are poorly understood and cell-type dependent [14]. In general, it is known that the ion conductivity G depends on the charge distribution across the membrane. However, it has been shown for PC12 cells that the membrane potential vanishes during swelling induced by a hyposmotic shock and it does not recover during the entire relaxation phase [14,15]. Hence, we assume a constant average G for simplicity and write the ion flux as

$$J_{\mathrm{ion}} = GkT \ln\frac{\phi_e}{\phi_i}. \tag{2}$$

The time variation of the internal number N of ions is $\dot{N} = J_{\mathrm{ion}}A$. Rescaling the conservation Eqs. (1) and (2) reveals two characteristic time scales: $\tau_w = \frac{R_0}{2L_p\Pi^0}$ for water influx and $\tau_{\mathrm{ion}} = \frac{\Pi^0 R_0}{2G(kT)^2}$ for ion conduction, where $\Pi^0 \approx 700$ kPa is the osmotic pressure of normal medium. For weak osmotic shocks the conservation Eqs. (1) and (2) can be linearized, resulting in a double exponential relaxation form for the volume, with characteristic time scales related to τ_w and τ_{ion}. At short times the volume change is given by $\Delta V = L_p\Delta\Pi_e A_0 t$, where $\Delta\Pi_e = \Delta\Pi(t = 0)$. Thus, the initial swelling is not influenced by elastic forces or ion flow. L_p measured from experiments increases from $L_p = 0.8 - 1.6(\pm 0.3) \times 10^{-14}$ m/(Pa · s), in a 15–37 °C range.

Numerical analysis of the volume response given by Eqs. (1) and (2) produces either a smaller swelling or a

longer relaxation as compared to experiments. To account for these, we consider the following biological processes. (i) The open probability of mechanosensitive ion channels increases with membrane tension [1]. Therefore, we expect an increase in ion conductivity upon swelling. Including a tension dependence on G, however, cannot account for the fast relaxation and large swelling. (ii) Filamentous actin undergoes a transient depolymerization mainly due to an influx of Ca^{2+} followed by repolymerization and contractility, due to myosin activation by Ca^{2+}, during volume relaxation [14,16]. Thus, this actin dynamics may account for both increased swelling and fast relaxation. Indeed, including an active pressure P_a in Eq. (1), after the maximum in volume, gives quantitative agreement with experiments as in Fig. 3(a). From the fits, we estimate $G = (0.7\text{–}4) \times 10^{38}/(\mathrm{J\,m^2\,s})$. Converting to electrical conductivity units gives $G \equiv 2\text{–}10\ \mathrm{S/m^2}$, in agreement with reported values [17]. We also estimate $P_a \sim (0.05\text{–}0.1)\Pi^0$. At sufficiently high temperatures, we often observe an ''undershoot'' of the volume (see Fig. 2), which could be attributed to active contraction of actin. This complex actin dynamics has not been reported for hyperosmotic shocks (sudden increase in external concentration). Indeed, the simpler analysis without active pressure fits well to our hyperosmotic shock data as shown in Fig. 3(b). Shrinking responses have previously been analyzed for kidney cells in suspension assuming volume dependent conductivities and neglecting elastic pressure [18].

Shape instability: As the neurite swells, the membrane tension σ increases, and for a critical swelling radius R_c it is unstable to peristaltic shape modulations. In [11] a scaling argument was developed to determine the fastest growing wavelength in cylindrical cells, assuming that dissipation is due to viscous flow inside the cell. Here, we take into account the gel-like structure of the neurite cytoskeleton. The solvent flow inside the gel is given by $-\nabla p + \eta\nabla^2\mathbf{v} - \zeta(\mathbf{v} - \partial_t\mathbf{u}) = 0$, where $\mathbf{v}$ is the solvent velocity ($\nabla\cdot\mathbf{v} = 0$), p the hydrodynamic pressure, $\mathbf{u}$ the gel elastic deformation, η the solvent viscosity, and ζ the gel-solvent friction. In addition, the gel elastic force is balanced by hydrodynamic friction $\zeta(\partial_t\mathbf{u} - \mathbf{v}) = \mu\nabla^2\mathbf{u} + (K + \frac{1}{3}\mu)\nabla(\nabla\cdot\mathbf{u})$. The solvent flow outside the neurite is given by the Stokes equations. We consider the stability of a modulation in the neurite radius $R = R_c + \epsilon e^{\omega t}\sin(qz)$, with amplitude ϵ and growth rate $\omega(q)$. We assume that the gel is in elastic equilibrium at the onset of the instability; i.e., radial compression modes have relaxed.

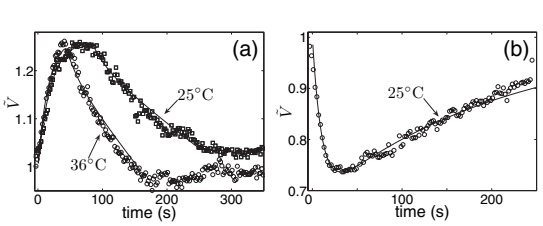

FIG. 3. Comparison between volume evolutions obtained experimentally and from the analysis. (a) For $\phi_0 \to 0.7\phi_0$ shock. $\tilde{K} = 0.025\Pi^0$, $P_a = 0.06\Pi^0$, $\tau_w = 22$ s, and $\tau_{\mathrm{ion}} = 70$ s for 25 °C. $\tilde{K} = 0.03\Pi^0$, $P_a = 0.09\Pi^0$, $\tau_w = 18$ s, and $\tau_{\mathrm{ion}} = 60$ s for 36° C. (b) For $0.5\phi_0 \to \phi_0$, using $\tilde{K} = 1.5\Pi^0$, $P_a = 0$, $\tau_w =$ 34 s, and $\tau_{\mathrm{ion}} = 24$. The neurite is densely filled with cytoskeleton and organelles that have to be compressed close to their ''dead volume'' for $V < V_0$, giving a higher effective value of K for (b).

The membrane imposes boundary conditions at the neurite surface. The solvent velocity is continuous, and the solvent flow through the membrane is governed locally by Eq. (1). The osmotic pressure difference is preserved within linear instability analysis, since a peristaltic modulation conserves volume to linear order. Conservation of membrane area implies $\partial_t u_r + R_c\partial_z v_z = 0$ [7]. The total radial stress jump (hydrodynamic and elastic) at the neurite surface must balance the Laplace pressure due to membrane tension $\Delta\sigma_{rr} = P_{\mathrm{Laplace}}$. Tangential force balance implies $\sigma^E_{rz} = \xi(v_z - \partial_t u_z)$, where σ^E is the gel elastic surface stress, and ξ the sliding friction coefficient between the cortical actin network and membrane. Rescaling the equations reveals two time scales for the gel dynamics: the relaxation time of compression modes, $\tau_C = \zeta R^2/K$, and that of shear modes $\tau_S = \eta/\mu$. The compression modes relax slower than the shear modes, $\tau_C \propto (R/\ell)^2\tau_S$, where ℓ is the mesh size of the gel. For a shear modulus $\mu \sim 1$ kPa and solvent viscosity 50 times water viscosity, $\tau_S \sim 10^{-4}$ s.

We find that the membrane-cytoskeleton sliding friction ξ affects the instability to order $\xi/(\zeta R)$. Assuming that the friction is due to anchored membrane proteins, and using common values for membrane viscosity, we estimate that $\xi \ll \zeta R$, showing that ξ can be neglected.

The neurite is unstable above a critical tension $\sigma_c = \frac{6K\mu R_c}{K+4/3\mu} + \mathcal{O}(\bar{q}^4)$. Close to σ_c the fastest growing wave number is $\bar{q} = qR_c = \sqrt{\frac{\sigma-\sigma_c}{2\sigma_c}}$ with a corresponding growth rate $\omega \sim \frac{1}{\tau_C}(\frac{\sigma-\sigma_c}{\sigma_c})^2$; thus, initially the dynamics is governed by the gel compression modes, which is qualitatively similar to the result in [8]. Above a second critical tension $\sigma_{c2} = 6\mu R_c$, the instability grows with the much faster rate $\omega \sim 1/\sqrt{\tau_S\tau_C}$. The tension σ_{c2} corresponds to the critical tension for pearling instability in an incompressible gel ($\sigma_c \to \sigma_{c2}$ when $K \to \infty$), which suggests that above σ_{c2} the instability grows via a peristaltic shear deformation of the gel. For high tension the fastest growing mode converges to the universal value $\bar{q} \approx 0.65$, independently of the gel elasticity and gel-solvent friction [see Fig. 4(a)].

Using $K \sim 20$ kPa, estimated from volume relaxation analysis, and $\mu \sim 1$ kPa [19] gives $\sigma_{c2} \approx 1.07\sigma_c$ and $\bar{q}_{c2} \approx 0.2$. For $R_0 \sim 0.5$ μm the critical tension for pearling is $\sigma_c \sim 3 \times 10^{-4}$ N/m.

The above analysis sets an upper limit $\bar{q} < 0.65$ on the fastest growing wave number, which is in good agreement with observations [see Figs. 4(a) and 4(b)]. Remarkably, we never observed wave numbers below $\bar{q} \lesssim 0.2$, even for dilutions close to the pearling threshold. This could be due

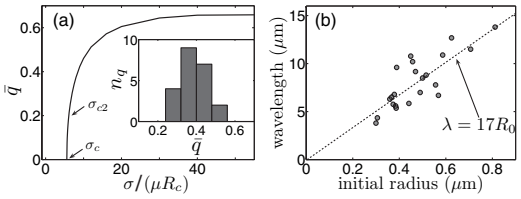

FIG. 4. (a) Theoretical plot for the fastest growing wave number with tension and histogram of observed wave numbers. (b) Variation of λ with R_0 at 25 °C for $\phi_0 \rightarrow 0.67\phi_0$. The scatter in the data is due to natural variations between cells.

to the steep increase in $\bar{q}$ close to σ_c. Also, the time scale for the growth of modes with small $\bar{q}$, which occur close to σ_c, may be longer than the volume regulation time, and hence these modes are not easily observable.

Surface area regulation: Figure 2 shows some remarkable features: (i) the instability begins to relax before the area, and hence the apparent tension, has reached its maximum value, (ii) the instability disappears when the measured area and volume are well above their values at its onset, and (iii) a 20% increase in area due to stretching alone is unexpected as most biological membranes are known to rupture beyond 3%–5% of stretching. A reasonable explanation for these observations is that lipids are continuously added to the membrane, thereby relaxing tension. Assuming that the membrane tension is the same at the onset and disappearance of the instability, we estimate a rate of increase of area of about 4×10^{-3} μm^2/s per unit length. This process would lead to a viscoelastic-like rate dependence of tension, giving rise to the critical rate of dilution mentioned earlier. The increase in area is most likely due to the fusion of tiny multilamellar vesicles to the outer membrane [20,21]. It is unlikely that this tension relaxation is due to flow of membrane from the extremities as (a) the onset and relaxation of the instability appear uniform along the length even in the longest neurites ($\sim$1 mm) and (b) we do not observe any flow of extraneous particles sticking to the outer membrane.

Conclusion.—Our experiments on the dynamics of the pearling instability in neurites reveal the role of volume regulatory mechanisms and direct membrane tension regulation in maintaining or recovering their normal cylindrical shape. Recovery to cylindrical shape has not been observed in previous experiments on beading cells. A possible explanation is that osmotic swelling is a gentle perturbation to which the cell has time to react before the deformation results in irreversible damage. Indeed, we observe that the instability is irreversible for sufficiently strong osmotic shocks. Moreover, it is not just the magnitude of osmotic swelling that triggers the instability, but also the rate at which the cell swells. Thus, observation of the instability is a direct way to probe the membrane surface regulation dynamics in neurites. We have also performed preliminary experiments on pulling neurites using a glass needle. There is a critical rate as well as magnitude of pulling beyond which peristaltic modes appear. For small amplitude modulations, the instability relaxes, whereas for strong modulations it persists. Physiologically, the volume and membrane surface regulation mechanisms should play an important role in stabilizing axon shape to sufficiently slow and gentle perturbations occurring *in vivo*. The theoretical analysis highlights the importance of cytoskeletal elasticity in the volume regulation processes and suggests that active contractions of the cytoskeleton may play an important role. The implications of our investigation to pathological conditions, especially to dendritic beading due to local inflammation [22], is an interesting topic for further research.

We are extremely grateful to J. Prost for valuable discussions and suggestions. Preliminary experiments were conducted at Institut Curie, Paris, where P. A. P. was supported by Institut Curie and CNRS. P. D. was supported by a Marie Curie fellowship. Financial support from the European Commission is acknowledged under Project No. HPRN-CT-2002-00312.

[1] B. Alberts *et al.*, *Molecular Biology of the Cell* (Garland Science Publishing, New York, 2002).
[2] C. J. Pike, B. J. Cummings, and C. W. Cotman, NeuroReport **3**, 769 (1992).
[3] P. Shannon *et al.*, Acta Neuropathol. **95**, 625 (1998).
[4] S. Ochs *et al.*, Prog. Neurobiol. **52**, 391 (1997).
[5] S. Al-Noori and J. Swann, Neuroscience (N.Y.) **101**, 337 (2000); D. Tanelian and V. Markin, Biophys. J. **72**, 1092 (1997).
[6] R. Bar-Ziv and E. Moses, Phys. Rev. Lett. **73**, 1392 (1994); R. Bar-Ziv, T. Tlusty, and E. Moses, Phys. Rev. Lett. **79**, 1158 (1997).
[7] P. Nelson, T. Powers, and U. Seifert, Phys. Rev. Lett. **74**, 3384 (1995).
[8] B. Barrière, K. Sekimoto, and L. Leibler, J. Chem. Phys. **105**, 1735 (1996).
[9] S. Chandrasekhar, *Hydrodynamic and Hydromagnetic Stability* (Dover, New York, 1981).
[10] V. S. Markin *et al.*, Biophys. J. **76**, 2852 (1999).
[11] R. Bar-Ziv *et al.*, Proc. Natl. Acad. Sci. U.S.A. **96**, 10 140 (1999).
[12] E. G. Banker and K. Goslin, *Culturing Nerve Cells* (MIT Press, Cambridge, MA, 1998).
[13] P. Agre and D. Kozono, FEBS Lett. **555**, 72 (2003).
[14] F. Lang *et al.*, Physiol. Rev. **78**, 247 (1998).
[15] M. Cornet, J. Ulb, and H. A. Kolb, J. Membr. Biol. **133**, 161 (1993).
[16] J. H. Henson, Microsc. Res. Tech. **47**, 155 (1999).
[17] T. F. Weiss, *Cellular Biophysics* (MIT Press, London, 1995), Vols. 1 and 2.
[18] A. D. Lúcio, R. A. S. Santos, and O. N. Mesquita, Phys. Rev. E **68**, 041906 (2003).
[19] B. Fabry *et al.*, Phys. Rev. Lett. **87**, 148102 (2001).
[20] Electron micrographs of PC12 cells show very few membrane invaginations, which could act as reservoirs [P. A. Pullarkat, A. Ott, and G. Acker (unpublished)].
[21] J. Dai *et al.*, J. Neurosci. **18**, 6681 (1998).
[22] B. Zhu *et al.*, Am. J. Pathol. **162**, 1639 (2003).